Theor Chem Acc (2012) 131:1179
DOI 10.1007/s00214-012-1179-x

REGULAR ARTICLE

Improving the study of proton transfers between amino acid side chains in solution: choosing appropriate DFT functionals and avoiding hidden pitfalls

Pedro J. Silva · Marta A. S. Perez · Natércia F. Brás · Pedro A. Fernandes · M. J. Ramos

Received: 24 September 2011 / Accepted: 2 November 2011 / Published online: 2 March 2012

Abstract We have studied the influence of implicit solvent models, inclusion of explicit water molecules, inclusion of vibrational effects, and density functionals on the quality of the predicted pK_a of small amino acid side chain models. We found that the inclusion of vibrational effects and explicit water molecules is crucial to improve the correlation between the computed and the experimental values. In these micro-solvated systems, the best agreement between DFT-computed electronic energies and benchmark values is afforded by BHHLYP and B97-2. However, approaching experimental results requires the addition of more than three explicit water molecules, which generates new problems related to the presence of multiple minima in the potential energy surface. It thus appears that a satisfactory ab initio prediction of amino acid side chain pK_a will require methods that sample the configurational space in the presence of large solvation shells, while at the same time computing vibrational contributions to the enthalpy and entropy of the system under study in all points of that surface. Pending development of efficient algorithms for those computations, we strongly suggest that whenever counterintuitive protonation states are found in a computational study (e.g., the presence of a neutral aspartate/neutral histidine dyad instead of a deprotonated aspartate/protonated histidine pair), the reaction profile should be computed under each of the different protonation microstates by constraining the relevant N–H or O–H bonds, in order to avoid artifacts inherent to the complex nature of the factors contributing to the pK_a.

Keywords DFT · Benchmarking · Acid/base reactions · Amino acid side chains

1 Introduction

The ubiquitous presence of protonation/deprotonation steps in the catalytic mechanisms of organic and biochemical reactions is responsible for the experimentally observed large effects of pH on many reaction rates. A good theoretical description of these reaction mechanisms, therefore, depends on the ability to predict accurately the solution pK_a of the reacting functional groups. Several protocols for computational determination of pK_a have been developed by several authors [1–6]. They all rely on the determination of gas phase reaction energies, followed by computation of solvation energies of the basic and acidic forms of the molecular species under study using implicit solvent models [1–3, 5, 6] or the Poisson equation [4], in the presence [2, 3, 5, 6] or absence [1, 4, 6] of a few explicit water molecules. The computed energy values are then converted to pK_a using appropriate thermodynamic cycles.

Dedicated to Professor Vincenzo Barone and published as part of the special collection of articles celebrating his 60th birthday.

Electronic supplementary material The online version of this article (doi:10.1007/s00214-012-1179-x) contains supplementary material, which is available to authorized users.

P. J. Silva
REQUIMTE/Faculdade de Ciências da Saúde, Universidade Fernando Pessoa, Rua Carlos da Maia, 296, 4200-150 Porto, Portugal

M. A. S. Perez · N. F. Brás · P. A. Fernandes · M. J. Ramos (✉)
REQUIMTE/Departamento de Química e Bioquímica, Faculdade de Ciências, Universidade do Porto, Rua do Campo Alegre, s/n, 4169-007 Porto, Portugal
e-mail: mjramos@fc.up.pt

Clearly, the quality of the results obtained critically depends on the accuracy of the individual computations performed in each step of the protocol, and this is reflected, for example, on the different correlations between computed and experimental values obtained for different classes of acids [7]. We have recently performed a thorough benchmarking study of the ability of 62 density functionals to accurately describe the proton affinity of large amino acid models [8]. However, to the best of our knowledge, no systematic study of the influence of each factor on the quality of the predicted pK_a values has been performed to date.

In this report, we describe the influence of: the implicit solvent model, inclusion of explicit water molecules, neglect of vibrational effects, and density functional used on the quality of predicted pK_a. We found that the inclusion of vibrational effects and explicit water molecules is crucial to improve the correlation between the computed and the experimental values. However, achieving convergence of the results requires the addition of too many explicit water molecules, which introduce new problems related to the presence of multiple minima in the potential energy surface. A satisfactory resolution of this problem will likely require ab initio methods capable of simultaneously addressing the presence of large solvation shells and the accurate computation of enthalpic/entropic effects.

2 Computational methods

The geometries of every molecule described were optimized at the MP2 level and with each of the tested density functionals. Autogenerated delocalized coordinates [9] were used in geometry optimizations performed with a medium-sized basis set, 6-31 + G (d), as increasing the basis sets to triple-ζ quality gives very small additional corrections to the geometries while dramatically increasing the computational cost [10–12]. Accurate DFT energies of the optimized geometries obtained with each density functional were then calculated using the same functional with several triple-ζ quality basis sets: 6-311 + G (d, p), 6-311 + G (2d, p), 6-311 + G (2d, 2p), and 6-311 + G (3d, 2p). We used 18 functionals in total—three GGA functionals (PBE96 [13, 14], PBEPW91 [13, 14] and PW91 [13]), eight hybrid-GGA functionals (B3LYP [15–17], B3PW91 [13, 15], B97-1 [18], B97-2 [19], BHHLYP (50% HF exchange + 50% B88 [20] exchange, with LYP correlation), PBE0 [21], PBE1PW91 [13, 14], and X3LYP [22]), three meta-GGA functionals (TPSS [23, 24], TPSSm [25], and M06-L [28]), and four meta-hybrid-GGA functionals (TPSSh [26], M06 [27], M06-2X [27], and M06-HF [29]). Functionals with dispersion corrections have been tried elsewhere to describe the proton affinity of large amino acid models [8] and found to generate very small dispersion effects. Computations involving CCSD (T), the B97-1, -2 and the M06 and TPSS families of functionals were performed with Gamess (US) [30]. All other computations were performed with the Firefly [31] quantum chemistry package. CCSD (T) and MP2 single-point energies were computed on the MP2 geometries using 6-31 + G (d), aug-cc-pVDZ and -pVTZ basis sets and extrapolated to the complete basis set limit as described by Schwenke [32] [for CCSD (T) level] or Truhlar [33, 34] (at the MP2 level). Comparison of these values to experimental free energies of protonation required the inclusion of the contribution of H^+ to the Gibbs free energy of the protonation reactions ($G_{gas,H+}$= −6.28 kcal mol^{-1} at 298 K and 1 atm) and the evaluation of zero-point and thermal effects on these geometries (computed from the MP2/6-31 + G (d) frequencies using a scaling factor of 0.967 [35]).

Since the computation of gas phase Gibbs free energies through any computational method entails the determination of the electronic energies and zero-point/vibrational energies (ZPVE) of each reactant and each product, the performance of a functional depends not only on the accuracy of the computed electronic energies but also on the quality of the vibrational frequencies provided by the method. In this work, we decided to focus on the electronic reaction energies *only*, to prevent spurious results arising from mutual cancellation of errors in energy/ZPVE, and because no ZPVE scaling factors are available for many of the method/basis set combinations tested. Basicities were computed as E_{acid}–E_{base}. DFT solvation energies were computed using the polarizable continuum model [36] implemented in each package [D-PCM [37, 38] in Firefly and C-PCM [39, 40] in Gamess (US)]. Average DFT solvation energies were used as estimates of MP2 solvation energies. For the solvation free energy of H^+, $G_{solv,H+}$, we used the value of −265.9 kcal mol^{-1}, obtained by converting the experimental value of −263.98 kcal mol^{-1} (Tissandier et al. [41]) to the appropriate thermodynamic standard state conventions as recommended by Kelly et al. [42].

Guanidine was selected as model for arginine acidities, and aspartate/glutamate and lysine were modeled as acetate and methylamine (respectively). Methanethiol was chosen to represent the cysteine side chain and phenol as tyrosine model. Histidine was modeled as methylimidazole. Both δ- and ε-deprotonated forms of methylimidazole were computed; all methods predicted the δ-deprotonated form to lie slightly lower in energy than the ε-deprotonated form. The average value for these protonations was used in all method comparisons, to avoid lending more weight to the histidine protonation versus other amino acids.

3 Results and discussion

3.1 Benchmarking selected density functionals in the gas phase

The energies of the selected set of model reactions range from −223.6 to −364.1 kcal mol^{-1} at the CCSD (T)/CBS//MP2/6-31 + G (d) level (Table 1). Energies predicted by MP2/CBS lie a few kcal mol^{-1} above CCSD (T)/CBS in all instances. Both theory levels agree very well with experimental results (Table 1) and can, therefore, be used as appropriate benchmarks for the density-functional theory computations. Interestingly, MP2/CBS agrees the most with experiment in the reactions involving a protonated and a neutral species, whereas CCSD (T) outperforms MP2/CBS in reactions involving a neutral and an anionic species.

Density-functional theory generally afforded geometries in very good agreement with MP2 geometries (root-mean-squared differences were most often below 0.02 Å). Large differences between functionals were only observed for the protonated arginine model: TPSS, TPSSm, PBE96, PBEPW91, and PW91 agree almost perfectly with the MP2 geometry (RMSD <0.015 Å), whereas BHHLYP places the hydrogens closer to the plane defined by the heavier atoms than the MP2 reference (RMSD = 0.077 Å); other functionals show RMSD versus MP2 between 0.02 and 0.05 Å. All tested functionals correctly predict the relative ordering of the gas phase reaction energies in this test set as dictated by experiment and CCSD (T)/CBS (with the exception of PBE96, PBEPW91, and PW91, which erroneously predict the protonation of the tyrosine model to be marginally less favorable than that of the aspartate model). The reaction energies obtained with the DFT functionals are generally overestimated relative to the CCSD (T)/CBS energies; B97-2 and BHHLYP are the major exceptions to this trend, as they underestimate all protonation energies (see Supporting Information).

3.2 Computing basicities in solution

Gas phase benchmark results are not directly applicable to the computation of reaction energies in solution because the amount of stabilization provided by the solvent depends on the amount of delocalized charge in the tested molecule. We, therefore, computed the reaction energies in solution for each of the reaction with every density functional, using the polarizable continuum model. As expected from simple charge considerations, the inclusion of solvent strongly favored the protonation of neutral species and disfavored the protonation of charged (anionic) species and, therefore, dramatically reduced the large spread of protonation energies, from −220/−360 kcal mol^{-1} in gas phase to −280/−306 kcal mol^{-1} in solution. However, the computed values correlate very poorly (or not at all) with the experimental trends: for example, aspartate is still predicted to be more basic than histidine (though much less so than in gas phase), irrespective of the polarizable continuum model used (either C-PCM [39, 40] or D-PCM [36] using an escaped charge compensation scheme [37, 38]) (Fig. 1, upper panel). Inclusion of zero-point and thermal effects does not improve these results.

Such poor performance of the PCM models conflicts with the usually good estimates of solvation energies they are able to provide [45]. Further analysis showed that this problem arises from the neglect of solvent-dependent stabilizing effects, since the inclusion of two explicit water molecules to the MP2 optimization of every system (or three water molecules in the case of the lysine and arginine models) greatly improves the correlation with experiment, though *only* upon addition of zero-point and thermal effects. Under these conditions, the correlation between computed and experimental values increases considerably (especially with the D-PCM solvation model) but still remains far below the desirable accuracy (Fig. 1, lower panel). Our attempts at systematic improvement of these results by expanding the micro-solvation spheres were

Table 1 Computed gas phase protonation energies of the amino acid side chain models

	Modeled amino acid	MP2/CBS	CCSD (T)/CBS	Experimental value of the model molecules
1.	Arginine	−239.9 (−**226.6**)	−242.6 (−**229.3**)	−226.9 [43]
2.	Aspartate	−352.6 (−**338.3**)	−356.1 (−**341.8**)	−341.4 ± 1.2 [44]
3.	Cysteine	−360.5 (−**348.3**)	−364.1 (−**351.8**)	−350.6 ± 2.0 [44]
4.	Histidine (δ-protonation)	−234.1 (−**218.4**)	−237.4 (−**221.7**)	−220.1 ± 2.0 [43]
5.	Histidine (ε-protonation)	−234.5 (−**219.6**)	−237.8 (−**222.9**)	
6.	Lysine	−221.6 (−**206.2**)	−223.6 (−**208.2**)	−206.6 ± 0.5 [43]
7.	Tyrosine	−354.4 (−**340.1**)	−358.1 (−**343.8**)	−342.9 ± 1.4 [44]

All values in kcal mol^{-1}. Bolded data in parentheses include zero-point energy, enthalpic and entropic contributions at 298.15 K computed at the MP2/6-31 + G (d) level and can be compared to the experimental ΔG values; conformational sampling was not needed to achieve experimental-quality results

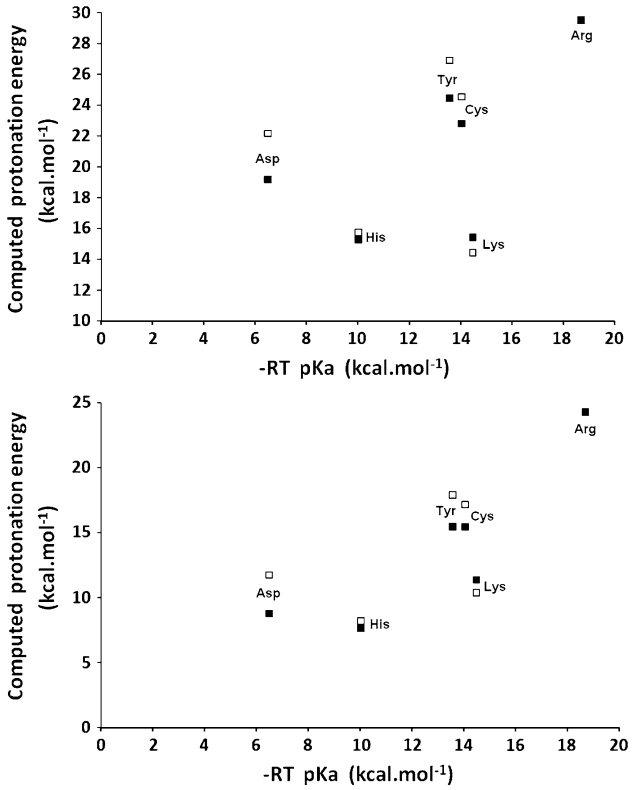

Fig. 1 Computed MP2/CBS protonation energy in solution versus experiment. *Filled square* solvation energies computed with D-PCM. *Open square* solvation energies computed with C-PCM. *Upper panel* without micro-solvation, ZPVE nor thermal effects. *Lower panel* including micro-solvation, ZPVE, and thermal effects

thwarted by the onset of difficulties regarding conformational sampling. This occurs because as the number of water molecules around the solute increases, so does the number of water–water interactions. In these small solute-water clusters, the change in the number of hydrogen bonds between the solute and the water as the solute becomes protonated often causes a dramatic reorganization of the water–water hydrogen bonds in the cluster, leading to large geometric rearrangements between the acidic and basic forms of the solute and misleading energy differences, that depend not only on the protonation energy itself, but also on the different regions of the potential energy surface of the solvent micro-cluster analyzed in each protonation state. The results above clearly show that attaining acceptable accuracy in the ab initio prediction of pK_a is prevented by the need to include a large solvation shell around the solutes, zero-point and vibrational effects throughout the potential energy surface, and sufficient conformational sampling to take into account each of the many local minima present in the potential energy surface. However, at least for biological systems in general, such large ab initio studies still lie beyond the reach of current computational technologies. It is, therefore, useful to identify the density functional(s) that more closely approach the MP2 results in micro-solvated systems for eventual application in DFT-based applications. We compared the MP2 micro-solvation behavior of the amino acid systems with density-functional theory by performing additional geometry optimizations with the explicitly solvated systems with each density functional, followed by computation of high-quality single-point energies in a polarizable continuum model. In all cases, the hydrogen bond lengths remain quite constant among methods, but due to the rotational flexibility of the added water molecules, the agreement between the obtained geometries and the MP2 geometries is substantially lower than observed in the water-free models. Root-mean squared deviations range from 0.17 Å (average value obtained with B3LYP or X3LYP) to 0.39 Å (average value obtained with M06). We found that whereas the precise implementation of the polarizable continuum model (either D- or C-PCM) affected the magnitude of solvation effect on the reaction energies, within each implementation, its effect was mostly independent of the precise geometry of the models (standard deviation of the continuum contribution to the reaction energies <0.7 kcal mol^{-1}). Since the increase in system size caused by the addition of explicit water molecules made CCSD (T) computations impractical, DFT-derived reaction energies were compared (Table 2) with the MP2/CBS benchmark, which has been shown above (Table 1) to provide overall deviations from experiment almost identical to those afforded by CCSD (T). Although most functionals afforded errors above 1.4 kcal mol^{-1} (≈ 1 pK_a unit), and two (B97-2 and BHHLYP) yielded large errors >5 kcal mol^{-1} (due to the systematic introduction of very similar errors in all reaction energies), three functionals (M06, M06-2X and PW91) yielded results very similar to the MP2 benchmark. Further analysis shows that the surprisingly large errors arise mostly from systematic underestimation (M06-HF, PBE0, PBE96, PW91, PBEPW91, and PBE1PW91) or overestimation (all other functionals, except M06-2X) of reaction energies. Many of these systematic errors cancel when the deprotonation energies of the amino acid models are compared with each other. Table 3 depicts the mean unsigned errors for the *differences* in reaction energies (which we call *relative* reaction energies) for all $6 \times 5/2$ reactions obtained by coupling any two acid/base pairs tested for each method, with the 6-311 + G (3d, 2p) basis sets. BHHLYP (MUE = 1.20 kcal mol^{-1}) and B97-2 (MUE = 1.35 kcal mol^{-1}) now emerge clearly as the best overall choices (closely followed by TPSSh). Much higher accuracy (MUE <0.4 kcal mol^{-1}) may, however, be obtained in selected cases involving proton transfer between only two amino acid side chains by using other functionals (Supporting information: Table S4).

Table 2 Mean unsigned errors in the computation of reaction energies with micro-solvated models using the 6-311 + G (3d, 2p) basis set

		MUE versus MP2/CBS
PBE96	GGA	2.11 ± 1.90
PBEPW91	GGA	2.01 ± 1.83
PW91	GGA	**1.34 ± 1.13**
B3LYP	Hybrid-GGA	1.91 ± 1.27
B3PW91	Hybrid-GGA	3.62 ± 1.35
B97-1	Hybrid-GGA	2.50 ± 1.43
B97-2	Hybrid-GGA	5.16 ± 1.11
BHHLYP	Hybrid-GGA	5.24 ± 1.12
PBE0	Hybrid-GGA	2.31 ± 1.28
PBE1PW91	Hybrid-GGA	1.96 ± 1.74
X3LYP	Hybrid-GGA	1.56 ± 1.17
TPSS	Meta-GGA	2.16 ± 1.13
TPSSm	Meta-GGA	2.32 ± 1.17
M06	Meta-hybrid-GGA	**1.34 ± 0.89**
M06-2X	Meta-hybrid-GGA	**1.35 ± 1.43**
M06-HF	Meta-hybrid-GGA	2.78 ± 2.35
M06-L	Meta-hybrid-GGA	3.72 ± 1.69
TPSSh	Meta-hybrid-GGA	3.24 ± 1.13

All values in kcal mol^{-1}. ZPVE not included. Error values below 1.5 kcal mol^{-1} are highlighted in bold

Table 3 Mean unsigned errors in the computation of reaction energy *differences* with micro-solvated models using the 6-311 + G (3d, 2p) basis set

		MUE versus MP2/CBS
PBE96	GGA	2.92 ± 1.76
PBEPW91	GGA	2.86 ± 1.73
PW91	GGA	1.97 ± 1.23
B3LYP	Hybrid-GGA	1.52 ± 0.99
B3PW91	Hybrid-GGA	1.65 ± 1.01
B97-1	Hybrid-GGA	1.85 ± 1.21
B97-2	Hybrid-GGA	**1.35 ± 0.83**
BHHLYP	Hybrid-GGA	**1.20 ± 1.06**
PBE0	Hybrid-GGA	2.00 ± 1.25
PBE1PW91	Hybrid-GGA	2.78 ± 1.69
X3LYP	Hybrid-GGA	**1.48 ± 1.00**
TPSS	Meta-GGA	1.52 ± 1.22
TPSSm	Meta-GGA	1.51 ± 1.21
M06	Meta-hybrid-GGA	1.77 ± 1.15
M06-2X	Meta-hybrid-GGA	2.18 ± 1.97
M06-HF	Meta-hybrid-GGA	2.73 ± 1.97
M06-L	Meta-hybrid-GGA	1.98 ± 1.40
TPSSh	Meta-hybrid-GGA	**1.26 ± 1.02**

All values in kcal mol^{-1}. ZPVE not included. Error values below 1.5 kcal mol^{-1} are highlighted in bold

4 Conclusions

It is clear from the results that, although in most cases a very satisfactory agreement between density functional theory and MP2 is found, the accuracy of the computed MP2 protonation energies in solution is still far from perfect, even with explicit micro-solvation of the chemical systems under study (Fig. 1). Preliminary trials revealed that improvement is unlikely to be achieved simply by a small increase in the number of explicit water molecules. Very large increases on the size of the solvent cluster, on the other hand, quickly take the problem out of reach of pure QM methodologies and further compound the problems due to the very large number of possible minima in the potential energy surface. The large effect of the zero-point and thermal effects on the quality of the correlations should also be kept in mind whenever proton transfer between amino acid side chains is studied, as these effects may reverse the computed relative basicities (e.g., using only electronic energies, lysine is predicted to be more acidic than histidine, whereas the inclusion of ZPVE and thermal effects results in the prediction of higher acidity of histidine relative to lysine). Since the computation of these vibrational contributions from the molecular hessian is only possible at stationary points, the full ab initio description of the free energy surface landscape must necessarily involve other methods of estimating entropic contributions at an ab initio level.

These confounding effects are probably at play in a number of theoretical studies that predict abnormal protonation behaviors, such as the predictions of a neutral aspartate/neutral histidine dyad instead of an anionic aspartate/cationic histidine [46–48], the proposal of an anionic histidine/neutral aspartate dyad in the reaction mechanism of Ca^{2+}-dependent phospholipase [49], or the prediction of neutral arginine/aspartic acid pairs instead of arginine/aspartate salt bridges [50]. We strongly suggest that whenever counterintuitive protonation states are found in a computational study, the reaction profile should be computed under the each of the different protonation micro-states by constraining the relevant N–H or O–H bonds. This strategy will provide a fuller understanding of the influence of each specific state of the relevant amino acid dyad on the reaction mechanism and avoid artifacts inherent to the complex nature of the factors contributing to the basicities of amino acid side chains.

References

1. da Silva CO, da Silva EC, Nascimento MAC (1999) J Phys Chem A 103:11194–11199

2. Adam KR (2002) J Phys Chem A 106:11963–11972
3. Pliego JR Jr, Riveros JM (2002) J Phys Chem A 106:7434–7439
4. Schmidt am Busch M, Knapp EW (2004) Chem Phys Chem 5:1513–1524
5. Kelly CP, Cramer CJ, Truhlar DG (2006) J Phys Chem A 110:2493–2499
6. Ho J, Coote ML (2010) Theor Chem Acc 125:3–21
7. Peräkylä M (1999) Phys Chem Chem Phys 1:5643–5647
8. Brás NF, Perez MAS, Fernandes PA, Silva PJ, Ramos MJ J Chem Theor Comp (submitted)
9. Baker J, Kessi A, Delley B (1996) J Chem Phys 105:192
10. Siegbahn PEM, Eriksson L, Himo F, Pavlov M (1998) J Phys Chem B 102:10622
11. Fernandes PA, Ramos MJ (2003) J Am Chem Soc 125:6311
12. Riley KE, Op't Holt BT, Merz KM Jr (2007) J Chem Theory Comput 3:407
13. Perdew JP (1991) Unified theory of exchange and correlation beyond the local density approximation. In: Ziesche P, Eschig H (eds) Electronic structure of solids '91. Akademie Verlag, Berlin, pp 11–20
14. Perdew JP, Burke K, Ernzerhof M (1996) Phys Rev Lett 77:3865
15. Becke AD (1993) J Chem Phys I(98):5648
16. Lee C, Yang W, Parr R (1998) J Phys Rev B 37:785
17. Hertwig RW, Koch W (1995) J Comp Chem 16:576
18. Hamprecht FA, Cohen AJ, Tozer DJ, Handy NC (1998) J Chem Phys 109:6264
19. Wilson PJ, Bradley TJ, Tozer DJ (2001) J Chem Phys 115:9233
20. Becke AD (1988) Phys Rev A 38:3098
21. Adamo C, Barone V (1999) J Chem Phys 110:6158
22. Xu X, Zhang Q, Muller RP, Goddard WA (2005) J Chem Phys 122:014105
23. Perdew JP, Tao J, Staroverov VN, Scuseria GE (2003) Phys Rev Lett 91:146401
24. Perdew JP, Tao J, Staroverov VN, Scuseria GE (2004) J Chem Phys 120:6898
25. Perdew JP, Ruzsinszky A, Tao J, Csonka GI, Scuseria GE (2007) Phys Rev A 76:042506
26. Staroverov VN, Scuseria GE, Tao J, Perdew JP (2003) J Chem Phys 119:12129 (erratum in J Chem Phys 121:11507)
27. Zhao Y, Truhlar DG (2008) Theor Chem Acc 120:215
28. Zhao Y, Truhlar DG (2006) J Chem Phys 125:194101
29. Zhao Y, Truhlar DG (2006) J Phys Chem A 110:13126
30. Schmidt MW, Baldridge KK, Boatz JA, Elbert ST, Gordon MS, Jensen JJ, Koseki S, Matsunaga N, Nguyen KA, Su S, Windus TL, Dupuis M, Montgomery JA (1993) J Comput Chem 14:1347
31. Granovsky AA Firefly version 7.0. http://classic.chem.msu.su/gran/gamess/index.html
32. Schwenke DW (2005) J Chem Phys 122:014107
33. Truhlar DG (1998) Chem Phys Lett 294:45
34. Zhao Y, Truhlar DG (2005) J Phys Chem A 109:6624
35. Merrick JP, Moran D, Radom L (2007) J Phys Chem A 111:11683–11700
36. Tomasi J, Persico M (1994) Chem Rev 94:2027–2094
37. Mennucci B, Tomasi J (1997) J Chem Phys 106:5151–5158
38. Cossi M, Mennucci B, Pitarch J, Tomasi J (1998) J Comput Chem 19:833–846
39. Barone V, Cossi M (1998) J Phys Chem A 102:1995–2001
40. Cossi M, Rega N, Scalmani G, Barone V (2003) J Comput Chem 24:669–681
41. Tissandier MD, Cowen KA, Feng WY, Gundluach E, Cohen MH, Earhart AD, Coe JV, Tuttle TR (1998) J Phys Chem A 102:7787–7794
42. Kelly CP, Cramer CJ, Truhlar DG (2006) J Phys Chem B 110:16066–16081
43. Hunter EP, Lias SG (1998) J Phys Chem Ref Data 27:413–656
44. Linstrom P, Mallard W (eds) (2003) NIST chemistry web book, NIST standard reference database number 69. National Institute of Standards and Technology, Gaithersburg. http://webbook.nist.gov
45. Barone V, Cossi M, Tomasi J (1997) J Chem Phys 107:3210–3221
46. Gómez PC, Pacios LF (2005) Chem Phys Phys Chem 7:1374–1381
47. Wang J, Dong H, Li H, He H (2005) J Phys Chem B 109:18664–18672
48. Schiøtt B (2004) Chem Commun, 498–499
49. Leopoldini M, Russo N, Toscano M (2010) J Phys Chem B 114:11584–11593
50. Nagy PI, Erhardt PW (2010) J Phys Chem B 114:16436–16442